X rays from relativistic electrons in a multilayer structure

N. N. Nasonov
Laboratory of Radiation Physics, Belgorod State University, 14 Studencheskaya str., Belgorod 308007, Russia

V. V. Kaplin and S. R. Uglov
Nuclear Physics Institute, Tomsk Polytechnic University, P.O. Box 25, Tomsk 634050, Russia

M. A. Piestrup and C. K. Gary
Adelphi Technology, Inc., 981B Industrial Road, San Carlos, California 94070, USA

A dynamic diffraction theory of x-ray emission by relativistic electrons crossing a finite-thickness multilayer mirror (e.g., alternating layers of W and B_4C) is developed, taking into account both diffracted transition and parametric radiation mechanisms. Simple formulas describing the characteristics of the total emission from either thin nonabsorbing or thick absorbing multilayers are derived. These formulas show that a multilayer radiator can be brighter and more efficient than crystalline ones. Good agreement between theory and prior experimental results is also shown. Thus the theory and its experimental verification demonstrate the possibility of a tunable quasimonochromatic x-ray source whose efficiency can be larger than that of other novel x-ray sources.

I. INTRODUCTION

When a relativistic electron crosses a single interface between two media with differing dielectric permeabilities, electromagnetic radiation is emitted as predicted by Ginzburg and Frank [1]. Known as transition radiation (TR), and considered as a possible bright source of x rays, this source has been studied both theoretically and experimentally [2–7]. TR's yield grows proportionally as the number of interfaces increases. Resonant transition radiation (RTR) can also occur when there is constructive interference of the waves emitted at these interfaces, resulting in a higher spectral-angular density [2,8–11]. Thin foils (e.g., Mylar) accurately spaced periodically in a vacuum have been used to produce RTR. For mechanical reason, the period of such structure cannot be smaller than a few microns. However, another possible RTR radiator is a periodic multilayer nanostructure, commonly known as a multilayer or x-ray mirror [12–19]. Such a structure can have much smaller medium periods, producing not only RTR, but also other processes. Indeed, if the multilayer is placed in the Bragg condition, the x rays can be scattered out and two processes, diffracted transition radiation (DTR) and parametric x-ray radiation (PXR), can occur by analogy with such emission processes in crystalline targets [3,20–27].

Since the period of the multilayer can be comparable to the wavelength of emitted photons, we go beyond the scope of the Wentzel-Kramers-Brillouin approximation, usually used in such analyses [3]. Different methods [14,15,17,18] were used earlier for the description of the emission processes in multilayer structures. In our opinion the most adequate approach to such a task is x-ray dynamic diffraction theory [28]. Previously, this approach, and its simple limit known as kinematic scattering theory (or perturbation theory), was used to describe PXR and DTR processes in crystalline targets [20,22,23,29,30].

As in Refs. [12,19] we use the dynamic diffraction theory to analyze the emission from relativistic electrons, crossing the multilayer. The main difference between our approach and that usually used in dynamic diffraction theory consists in the separation of the total emission amplitude into PXR and DTR amplitudes (see Refs. [31,32]). Such an approach allows to elucidate in more detail the relation between PXR and DTR relative contributions to the formation of total emission yield (among other things this question is of importance because DTR contribution has been not considered in Refs. [12,19]).

The general case of multilayered structures with a finite thickness is considered here for two reasons. First, the number of multilayers are limited in number (e.g., $N<300$) due to deposition problems and errors, thus limiting the overall multilayer thickness. Second, PXR and DTR yields have differing dependencies on multilayer thickness. DTR yield is not proportional to the thickness in contrast with PXR; hence, an optimal thickness of the multilayer can be derived.

The main goal of this work is to substantiate the advantage of the multilayer as a radiator for intense tunable x-ray production as compared with a crystalline target. Experimental studies of x-ray emission from relativistic electrons passing through a multilayer nanostructure have been performed recently [33]. One of the aims of this work is to give a theoretical explanation for these results [33].

II. THE TOTAL EMISSION AMPLITUDE

We will first determine the electromagnetic field emitted by a relativistic electron moving in a medium with periodic dielectric susceptibility $\chi(\omega,\mathbf{r})=\chi_0(\omega)+\Sigma_{\mathbf{g}}{}'\chi_{\mathbf{g}}(\omega)\,e^{i\mathbf{g}\cdot\mathbf{r}}$. In the case of a one-dimensional structure consisting of alternative layers with thicknesses a and b and susceptibilities

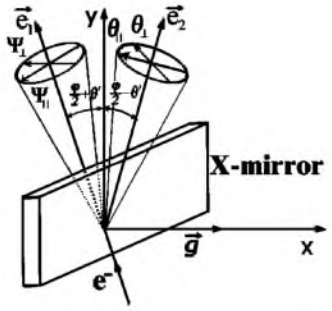

FIG. 1. The geometry of the emission process. A multilayer mirror is positioned at the Bragg condition in an electron beam to generate x rays. $\mathbf{g}$ is the reciprocal-lattice vector, $\mathbf{e}_1$ is the electron-beam axis, $\mathbf{e}_2$ is the photon collimator axis, φ is the emission angle, θ' is the orientational angle, which may be changed by the goniometer, $\Theta_{\|}$ and $\Psi_{\|}$ are the components of the angular variables $\boldsymbol{\Theta}$ and $\boldsymbol{\Psi}$ parallel to the plane determined by the vectors $\mathbf{e}_1$ and $\mathbf{e}_2$, $\Theta_{\perp}$ and $\Psi_{\perp}$ are the components perpendicular to such a plane.

$\chi_a(\omega)$ and $\chi_b(\omega)$, respectively, the quantities $\chi_0(\omega)$ and $\chi_{\mathbf{g}}(\omega)$ are determined by the expressions

$$\chi_0(\omega)=\frac{a}{T}\chi_a+\frac{b}{T}\chi_b,$$

$$\chi_{\mathbf{g}}(\omega)=\frac{1-e^{i\mathbf{g}\cdot\mathbf{a}}}{igT}(\chi_a-\chi_b), \tag{1}$$

where $T=a+b$ is the period of multilayered structure, $\mathbf{g}=\mathbf{e}_x g$, $g\equiv g_n=(2\pi/T)n$, $n=0,\pm1,\pm2,\ldots$, $\mathbf{e}_x$ is the normal to the surface of a layer (see Fig. 1). The Fourier transform of the electric field

$$\mathbf{E}_{\omega\mathbf{k}}=(2\pi)^{-4}\int d^3r dt e^{-i\mathbf{k}\cdot\mathbf{r}+i\omega t}\mathbf{E}(\mathbf{r},t)$$

is determined by means of the ordinary Maxwell equation

$$(k^2-\omega^2)\mathbf{E}_{\omega\mathbf{k}}-\mathbf{k}(\mathbf{k}\cdot\mathbf{E}_{\omega\mathbf{k}})-\omega^2\chi_0\mathbf{E}_{\omega\mathbf{k}}-\omega^2{\sum_{\mathbf{g}}}'\chi_{-\mathbf{g}}\mathbf{E}_{\omega\mathbf{k}+\mathbf{g}}$$
$$=\frac{i\omega e}{2\pi^2}\mathbf{v}\delta(\omega-\mathbf{k}\cdot\mathbf{v}), \tag{2}$$

where $\mathbf{v}$ is the emitting particle velocity. Since χ_0, $\chi_{\mathbf{g}}\ll1$ for x rays, the solution of Eq. (2) may be obtained from two-wave approximation of the dynamic diffraction theory [28]. Taking into account that the field components $\mathbf{E}_{\omega\mathbf{k}}$ and $\mathbf{E}_{\omega\mathbf{k}+\mathbf{g}}$ are approximately transverse to the vectors $\mathbf{k}$ and $\mathbf{k}+\mathbf{g}$, respectively [34], we reduce Eq. (2) to two well known equations:

$$(k^2-\omega^2-\omega^2\chi_0)E_{\lambda0}-\omega^2\chi_{-\mathbf{g}}\alpha_\lambda E_{\lambda\mathbf{g}}$$
$$=\frac{i\omega e}{2\pi^2}\mathbf{e}_{\lambda0}\cdot\mathbf{v}\delta(\omega-\mathbf{k}\cdot\mathbf{v}), \tag{3a}$$

$$[(\mathbf{k}+\mathbf{g})^2-\omega^2-\omega^2\chi_0]\mathbf{E}_{\lambda\mathbf{g}}-\omega^2\chi_{\mathbf{g}}\alpha_\lambda\mathbf{E}_{\lambda0}=0, \tag{3b}$$

where new quantities have been defined by the expressions

$$\mathbf{E}_{\omega\mathbf{k}}=\sum_{\lambda=1}^{2}\mathbf{e}_{\lambda0}E_{\lambda0},\quad \mathbf{E}_{\omega\mathbf{k}+\mathbf{g}}=\sum_{\lambda=1}^{2}\mathbf{e}_{\lambda\mathbf{g}}E_{\lambda\mathbf{g}},$$

$$\mathbf{e}_{10}=\mathbf{e}_{1\mathbf{g}}=\frac{[\mathbf{k}_{\|},\mathbf{e}_x]}{k_{\|}},\quad \mathbf{e}_{20}=\frac{[\mathbf{k},\mathbf{e}_{20}]}{k},\quad \mathbf{e}_{2\mathbf{g}}=\frac{[\mathbf{k}+\mathbf{g},\mathbf{e}_{20}]}{|\mathbf{k}+\mathbf{g}|}, \tag{4}$$

$$\alpha_1=1,\quad \alpha_2=\mathbf{k}\cdot(\mathbf{k}+\mathbf{g})/k|\mathbf{k}+\mathbf{g}|,$$

$$\mathbf{k}=\mathbf{e}_x k_x+\mathbf{k}_{\|},\quad \mathbf{e}_x\cdot\mathbf{k}_{\|}=0.$$

Equations (3) describe the electromagnetic field inside the multilayer. The corresponding wave equations for field components $E^V_{\lambda0}$ and $E^V_{\lambda\mathbf{g}}$ in the vacuum outside the multilayer follow from Eq. (3) in the limit $\chi_0=\chi_{\mathbf{g}}=0$. Since only the Bragg geometry can be realized for a multilayer (Laue geometry for a multilayer is mechanically impossible at this time), it is sufficient to determine the components $E^V_{\lambda0}$ and $E^V_{\lambda\mathbf{g}}$ in the vacuum in front of the multilayer (region $x>0$ in Fig. 1). Using the general expressions for the field components $E_{\lambda0,\mathbf{g}}$ and $E^V_{\lambda0,\mathbf{g}}$ following from corresponding wave equations (for example, most interesting for us solution

$$E^V_{\lambda\mathbf{g}}=a_{\lambda\mathbf{k}_{\|}}\delta(k_{gx}-p),\quad p=\sqrt{\omega^2-k_{\|}^2},\quad k_{gx}=k_x+g \tag{5}$$

describes the emission field in a vacuum) and ordinary boundary conditions for electromagnetic fields on front and back surfaces of the multilayer,

$$\int dk_x(E_{\lambda0}-E^V_{\lambda0})=\int dk_x e^{-ik_xL}E_{\lambda\mathbf{g}}=\int dk_x(E_{\lambda g}-E^V_{\lambda g})$$
$$=0, \tag{6}$$

we can determine the coefficient $a_{\lambda\mathbf{k}_{\|}}$. Since solving this equation is the standard task of dynamic diffraction theory, we present the final result only,

$$a_{\lambda\mathbf{k}_{\|}}=\frac{i\omega^3 e\chi_{\mathbf{g}}\alpha_\lambda\mathbf{e}_{\lambda0}\cdot\mathbf{v}}{8\pi^2p^2|v_x|}\frac{A}{B},$$

$$A=\left(\frac{1}{\Delta_0}-\frac{1}{\Delta_1-\xi_1}\right)(1-e^{-i(\Delta_1-\xi_1)L})-\left(\frac{1}{\Delta_0}-\frac{1}{\Delta_1-\xi_2}\right)(1$$
$$-e^{-i(\Delta_1-\xi_2)L}), \tag{7}$$

$$B=\xi_2e^{-i(\Delta_1-\xi_2)L}-\xi_1e^{-i(\Delta_2-\xi_1)L},$$

where the following designations are used:

$$\Delta_0=\frac{1}{|v_x|}(\omega-\mathbf{k}_{||}\cdot\mathbf{v}_{||}-p|v_x|),\quad \Delta_1=\Delta_0-\frac{\omega^2}{2p}\chi_0,$$

$$\xi_{1,2}=\frac{1}{2}\left(\Delta'\pm\sqrt{\Delta'^2-\frac{\omega^4}{p^2}\chi_{\mathbf{g}}\chi_{-\mathbf{g}}\alpha_\lambda^2}\right),$$

$$\Delta'=\Delta-\frac{\omega^2}{p}\chi_0,\quad \Delta=g\left(\frac{g}{2p}-1\right). \tag{8}$$

An influence of dynamic diffraction effects on the emission properties is described in the general solution (7) by the variables Δ and $\xi_{1,2}$ (such an influence may be essential if $\Delta^2\leqslant\omega^4/p^2\chi_{\mathbf{g}}\chi_{-\mathbf{g}}\alpha_\lambda^2$). The quantities $\xi_{1,2}$ determine two different solutions of dispersion equation $k_{gx}=k_{gx}^{(1,2)}\equiv p+\omega^2/2p\chi_0+\xi_{1,2}$, and Δ is the so-called resonance defect, describing the deviation of emitted photons from the exact Bragg resonance.

To determine the emission amplitude A_λ, we calculate the Fourier integral

$$E_\lambda^{rad}=\int d^3k_g e^{i\mathbf{k}_\mathbf{g}\cdot\mathbf{n}r}E_{\lambda\mathbf{g}}^V, \tag{9}$$

where $\mathbf{n}$ is the unit vector in the direction of emitted photon propagation. The field E_λ^{Rad} in the wave zone is calculated by the stationary-phase method:

$$E_\lambda^{rad}=A_\lambda\frac{e^{i\omega r}}{r},\quad A_\lambda=-2\pi i\omega n_x a_{\lambda\,\omega\mathbf{n}_{||}}, \tag{10}$$

where $\mathbf{n}=\mathbf{n}_{||}+\mathbf{e}_x n_x$, $\mathbf{e}_x\cdot\mathbf{n}_{||}=0$.

Expressions (7), (8), and (10) give a detailed description of the emission amplitude A_λ. To simplify the obtained result we define the angular variables $\boldsymbol{\Theta}$ and $\boldsymbol{\Psi}$ in accordance with the formulas

$$\mathbf{v}=\mathbf{e}_1\left(1-\frac{1}{2}\gamma^{-2}-\frac{1}{2}\Psi^2\right)+\boldsymbol{\Psi},\quad \mathbf{e}_1\cdot\boldsymbol{\Psi}=0, \tag{11a}$$

$$\mathbf{n}=\mathbf{e}_2\left(1-\frac{1}{2}\Theta^2\right)+\boldsymbol{\Theta},\quad \mathbf{e}_2\cdot\boldsymbol{\Theta}=0,\quad \mathbf{e}_1\cdot\mathbf{e}_2=\cos\varphi, \tag{11b}$$

were γ is the Lorentz factor of an emitting particle. The components of the angular variables $\boldsymbol{\Psi}=\boldsymbol{\Psi}_{||}+\boldsymbol{\Psi}_\perp$, $\boldsymbol{\Psi}_\perp\cdot\boldsymbol{\Psi}_{||}=0$ and $\boldsymbol{\Theta}=\boldsymbol{\Theta}_{||}+\boldsymbol{\Theta}_\perp$, $\boldsymbol{\Theta}_\perp\cdot\boldsymbol{\Theta}_{||}=0$ are shown in Fig. 1. In addition to this, it is very convenient to separate the total amplitude A_λ into two components: a PXR emission amplitude A_λ^{PXR} and a DTR emission amplitude A_λ^{DTR}.

The final expression for emission amplitude A_λ has a form

$$A_\lambda=A_\lambda^{PXR}+A_\lambda^{DTR}, \tag{12a}$$

$$A_\lambda^{PXR}=\frac{e\omega^2\chi_{\mathbf{g}}\alpha_\lambda}{4\pi\sin^2(\varphi/2)}\frac{\mathbf{e}_{\lambda0}\cdot\mathbf{v}}{\xi_2e^{-i(\Delta_1-\xi_2)L}-\xi_1e^{-i(\Delta_1-\xi_1)L}}\times\left[\frac{\xi_2}{\Delta_1}\frac{1-e^{-i(\Delta_1-\xi_2)L}}{\Delta_1-\xi_2}-\frac{\xi_1}{\Delta_1}\frac{1-e^{-i(\Delta_1-\xi_1)L}}{\Delta_1-\xi_1}\right], \tag{12b}$$

$$A_\lambda^{DTR}=\frac{e\omega^2\chi_{\mathbf{g}}\alpha_\lambda}{4\pi\sin^2(\varphi/2)}\mathbf{e}_{\lambda0}\cdot\mathbf{v}\left[\frac{1}{\Delta_0}-\frac{1}{\Delta_1}\right]\frac{e^{i\xi_2L}-e^{i\xi_1L}}{\xi_2e^{i\xi_2L}-\xi_1e^{i\xi_1L}}, \tag{12c}$$

where the quantities Δ_0, Δ_1, and Δ' appearing in Eq. (12) and defined above by Eqs. (8) can be presented as

$$\Delta_0=\frac{\omega}{2\sin(\varphi/2)}[\gamma^{-2}+(\Theta_\perp-\Psi_\perp)^2+(2\theta'+\Theta_{||}+\Psi_{||})^2],\quad \Delta_1=\Delta_0-\frac{\omega}{2\sin(\varphi/2)}\chi_0,$$

$$\Delta'=g\left[\frac{\omega_B'}{\omega}-1-\frac{\chi_0}{2\sin^2(\varphi/2)}\right]\approx g\left(\frac{\omega_B'}{\omega}-1\right)\equiv\Delta. \tag{13}$$

The important quantity ω_B' in Eq. (13),

$$\omega_B'=\omega_B\left[1+(\theta'+\Theta_{||})\cot\left(\frac{\varphi}{2}\right)\right],\quad \omega_B=\frac{g}{2\sin(\varphi/2)}, \tag{14}$$

where ω_B is the Bragg frequency, in the vicinity of which the emission is concentrated, describes the dependence of characteristic energy of emitted photons on both the orientation angle θ' (this angle is subject to wide variations by the goniometer in which the multilayer is installed) and the observation angle $\Theta_{||}$.

The quantities Δ_0L and Δ_1L are the ratios of an emitting electron path in the multilayer $L/\sin(\varphi/2)$ to emission formation length in (1) a vacuum and in (2) a medium with the average dielectric susceptibility χ_0, respectively.

Result (12) now allows us to (1) compare the efficiencies of multilayer and crystalline radiators, (2) estimate the relative DTR and PXR contributions to total emission yield for various parameter ranges, and (3) compare theory with the prior experimental results [33].

III. THE EMISSION PROPERTIES

Let us consider first the DTR contribution from a thin target with a thickness smaller than the photoabsorption length. The expression for DTR spectral-angular distribution follows from Eq. (12c):

$$\omega\frac{dN_\lambda^{DTR}}{d\omega d^2\Theta}=\frac{e^2}{\pi^2}\left\langle\Omega_\lambda^2\left(\frac{1}{\gamma^{-2}+\Omega^2}-\frac{1}{\gamma^{-2}-\chi_0+\Omega^2}\right)^2\right\rangle R_\lambda^{DTR}(t_\lambda,\tau_\lambda),\quad(15a)$$

$$R_\lambda^{DTR}=\frac{|\sin(t_\lambda\sqrt{\tau_\lambda^2-1})|^2}{|\tau_\lambda^2-1|+|\sin(t_\lambda\sqrt{\tau_\lambda^2-1})|^2},\qquad(15b)$$

where $\Omega_1=\Theta_\perp-\Psi_\perp$, $\Omega_2=2\theta'+\Theta_\parallel+\Psi_\parallel$, $\Omega^2=\Omega_1^2+\Omega_2^2$, the brackets $\langle\ \rangle$ mean the averaging over the angles $\Psi_\perp$ and $\Psi_\parallel$, describing an angular spread in the beam of emitting electrons, the coefficient t_λ and the function $\tau_\lambda(\omega)$ are defined by the formulas

$$t_\lambda=\frac{\omega|\chi_{\mathbf{g}}|L\alpha_\lambda}{2\sin(\varphi/2)},\quad\tau_\lambda(\omega)=\frac{2\sin^2(\varphi/2)}{|\chi_{\mathbf{g}}|\alpha_\lambda}\left(1-\frac{\omega}{\omega_B'}\right).\qquad(16)$$

Physical meanings of these quantities are as follows: t_λ is half of the ratio of electron path in the target $L/\sin(\varphi/2)$ to extinction length $1/\omega|\chi_{\mathbf{g}}|\alpha_\lambda$, and the rapidly changing variable $\tau_\lambda(\omega)$ is the ratio of the resonance defect Δ to the width of Bragg resonance $\omega|\chi_{\mathbf{g}}|\alpha_\lambda/\sin(\varphi/2)$.

Result (15) shows that DTR arises due to dynamic scattering of the transition radiation, emitted by a relativistic electron from the front surface of the multilayer. The front half of Eq. (15a) describes single-interface transition radiation [1], while R_λ^{DTR} in Eq. (15b) is a reflection coefficient. From Eq. (15b) the function R_λ^{DTR} decreases proportional to τ_λ^{-2} outside the narrow frequency range close to the Bragg frequency ω_B, where $|\tau_\lambda(\omega)|<1$ and an anomalous dispersion for x rays is realized. As a consequence DTR spectral width has a value of about $\Delta\omega/\omega\approx|\chi_{\mathbf{g}}|\alpha_\lambda/2\sin^2(\varphi/2)$.

The formula for the DTR photon number follows from Eqs. (15) after integrating over ω and $\mathbf{\Theta}$ [when integrating over ω one should take into account that only the fast variable $\tau_\lambda(\omega)$ may be changed essentially in Eqs. (15)], and has a simple form

$$N_\lambda^{DTR}=\frac{e^2|\chi_{\mathbf{g}}|\alpha_\lambda}{8\sin^2(\varphi/2)}\tanh(t_\lambda)\left[\left(1+2\frac{\gamma_*^2}{\gamma^2}\right)\times\ln\left(\frac{(1+\gamma^2\Theta_d^2)(1+\gamma^2/\gamma_*^2)}{1+\gamma^2\Theta_d^2+\gamma^2/\gamma_*^2}\right)-\frac{\gamma^2\Theta_d^2}{1+\gamma^2\Theta_d^2}-\frac{\gamma^2\Theta_d^2}{1+\gamma^2\Theta_d^2+\gamma^2/\gamma_*^2}\right],\qquad(17)$$

where Θ_d is the photon collimator angular size, and the quantity γ_* is defined by $\chi_0=-\langle\omega_p^2\rangle/\omega^2\approx-\langle\omega_p^2\rangle/\omega_B^2\equiv-\gamma_*^{-2}$ ($\langle\omega_p^2\rangle$ is the average plasma frequency of the multilayer).

Since the target dielectric characteristics are presented in Eq. (17) by the quantities χ_0 and $|\chi_{\mathbf{g}}|$ only, one can use the result to describe arbitrary targets with periodic dielectric susceptibilities including crystals. Let us compare crystalline and multilayer DTR radiators. Assuming the Bragg frequency ω_B to be far from absorption edges for the target material, we introduce the quantity $\omega_{\mathbf{g}}^2$ so that $|\chi_{\mathbf{g}}|=\omega_{\mathbf{g}}^2/\omega^2\approx\omega_{\mathbf{g}}^2/\omega_B^2$. For example, $\omega_{\mathbf{g}}^2=\langle\omega_p^2\rangle F(\mathbf{g})|S(\mathbf{g})|e^{-g^2u_T^2/2}$ for a crystal [$F(\mathbf{g})$ is the atom form factor, $S(\mathbf{g})$ is the structure factor of an elementary cell, u_T is the mean square amplitude of atom thermal vibrations] and

$$\omega_{\mathbf{g}}^2=(\omega_a^2-\omega_b^2)\frac{\sin\left(\pi\frac{a}{T}\right)}{\pi}$$

for the multilayer in accordance with Eq. (1). The ratio of DTR yield from a crystal to that from a multilayer is

$$\frac{N_{\lambda(cr)}^{DTR}}{N_{\lambda(mir)}^{DTR}}=\frac{\omega_{\mathbf{g}(cr)}^2\alpha_{\lambda(cr)}}{\omega_{\mathbf{g}(mir)}^2\alpha_{\lambda(mir)}}\frac{T_{(cr)}^2}{T_{(mir)}^2}=\frac{\Delta\omega_{(cr)}^{DTR}}{\Delta\omega_{(mir)}^{DTR}},\qquad(18)$$

following from Eq. (17) on condition of a thick target ($t_\lambda=\omega_{\mathbf{g}}^2T^2\alpha_\lambda/2\pi M\equiv M/M_{opt}>1$, M is the number of periods in the radiator) and high electron energies ($\gamma>\gamma_*$). Here $T=2\pi/g$ is the period of the radiator. Since the quantities $\omega_{\mathbf{g}(cr)}^2$ and $\omega_{\mathbf{g}(mir)}^2$ are comparable (see above definitions), Eq. (18) predicts a higher efficiency of a multilayer as a DTR radiator relative to that of a crystal radiator, since $T_{(mir)}$ exceeds $T_{(cr)}$. On the other hand, Eq. (18) shows that the spectral width of DTR flux emitted from the crystalline radiator is smaller than that from the multilayer.

We obtain the PXR spectral-angular distribution from Eq. (12b) by noting that only one term is proportional to $(\Delta_1-\xi_1)^{-1}$ and makes the important contribution since on the equality $\mathrm{Re}(\Delta_1-\xi_1)=0$ may be valid:

$$\omega\frac{dN_\lambda^{PXR}}{d\omega d^2\Theta}=\frac{e^2}{\pi^2}\left\langle\frac{\Omega_\lambda^2}{(\gamma^{-2}-\chi_0+\Omega^2)^2}R_\lambda^{PXR}\right\rangle,\qquad(19a)$$

$$R_\lambda^{PXR}=\frac{(\tau_\lambda+\sqrt{\tau_\lambda^2-1})^2}{\tau_\lambda^2-1+\sin^2(t_\lambda\sqrt{\tau_\lambda^2-1})}\times\frac{\sin^2\left[\frac{1}{2}t_\lambda\{\tau_\lambda+\sqrt{\tau_\lambda^2-1}-(\gamma^{-2}-\chi_0+\Omega^2)/|\chi_{\mathbf{g}}|\alpha_\lambda\}\right]}{[\tau_\lambda+\sqrt{\tau_\lambda^2-1}-(\gamma^{-2}-\chi_0+\Omega^2)/|\chi_{\mathbf{g}}|\alpha_\lambda]^2},\qquad(19b)$$

analogous to Eqs. (15).

Equation (19) explains PXR as a process of coherent scattering of the screened Coulomb field of a relativistic electron moving in a medium with the average dielectric permeability $\epsilon(\omega)=1+\chi_0(\omega)$. In the case of a thick target ($t_\lambda=\omega_{\mathbf{g}}^2T^2\alpha_\lambda/2\pi M\gg1$) the reflection coefficient R_λ^{PXR} has a sharp maximum at the point $\tau_\lambda=\tau_{\lambda*}=1+(\gamma^{-2}+\gamma_*^{-2}+\Omega^2-|\chi_{\mathbf{g}}|\alpha_\lambda)^2/2(\gamma^{-2}+\gamma_*^{-2}+\Omega^2)|\chi_{\mathbf{g}}|\alpha_\lambda>1$ placed outside the range of anomalous dispersion where $|\tau_\lambda|<1$ and DTR dominates.

Distribution (19) can be integrated over ω for the practical case $t_\lambda \gg 1$ by using the approximation $\sin^2(tx)/x^2 \to \pi t\delta(x)$. The result of integrating,

$$\frac{N_\lambda^{PXR}}{d^2\Theta} = \frac{e^2}{\pi^2}\left(\frac{\omega_g^2 T^2 \alpha_\lambda}{2\pi}\right)^2 M\left\langle \frac{\Omega_\lambda^2}{(\gamma^{-2}+\gamma_*^{-2}+\Omega^2)^2 - |\chi_g|^2\alpha_\lambda^2} \times\left[1+\frac{4(\gamma^{-2}+\gamma_*^{-2}+\Omega^2)^2|\chi_g|^2\alpha_\lambda^2}{[(\gamma^{-2}+\gamma_*^{-2}+\Omega^2)^2-|\chi_g|^2\alpha_\lambda^2]^2} \times\sin^2\left(t_\lambda\frac{(\gamma^{-2}+\gamma_*^{-2}+\Omega^2)^2-|\chi_g|^2\alpha_\lambda^2}{2(\gamma^{-2}+\gamma_*^{-2}+\Omega^2)|\chi_g|\alpha_\lambda}\right)\right]^{-1}\right\rangle, \tag{20}$$

allows us not only to compare the efficiencies of PXR radiators using either a crystal or a multilayer, but also to estimate an influence of dynamic diffraction effects on PXR properties as well.

Since PXR yield is proportional to the target thickness $L = TM$, the yields from the mirror and crystal radiators with equal thicknesses can be compared. The corresponding formula

$$\frac{N_{\lambda(cr)}^{PXR}}{N_{\lambda(mir)}^{PXR}} \approx \frac{\omega_{g(cr)}^4 \alpha_{\lambda(cr)}^2}{\omega_{g(mir)}^4 \alpha_{\lambda(mir)}^2}\frac{T_{(cr)}^3}{T_{(mir)}^3} \tag{21}$$

shows the higher yield of the multilayer as a PXR source using the above same arguments that were used concerning Eq. (18).

To determine the possibilities of a multilayer as a radiator we should compare the relative PXR and DTR contributions. Let us first consider the influence of dynamic diffraction effects on PXR (this question is of the great interest since there is no consensus on such an influence) and the interference between these two emission mechanisms. From Eq. (20) the dynamic diffraction effects may be important for high electron energies $\gamma \gg \gamma_*$ only, but an added condition $\omega_g^2/\langle\omega_p^2\rangle \equiv q \approx 1$ must also be fulfilled for such effects to happen. Analysis has shown the occurrence of strong oscillations in PXR angular distribution (20) for the conditions $\gamma \gg \gamma_*$ and $q \approx 1$. The latter

$$q = \frac{\sin\left(\pi\frac{a}{T}\right)}{\pi\frac{a}{T}}\frac{1-\omega_b^2/\omega_a^2}{1+\omega_b^2(T-a)/\omega_a^2 a} \approx 1$$

may be fulfilled with the proviso that $\omega_b^2 \ll \omega_a^2$ and $a \ll T$. On the other hand, the relation $a = \frac{1}{2}T$ is best suited to x-ray production by a multilayer because DTR and PXR yields are proportional to $\sin(\pi a/T)$ and $\sin^2(\pi a/T)$ in accordance with Eqs. (17) and (20). As this takes place $q < 2/\pi$ and therefore an influence of dynamical diffraction effects is small for the most practical case.

With this conclusion PXR yield follows from Eq. (20) in the form

$$N_\lambda^{PXR} = \frac{e^2}{2\pi}\left(\frac{\omega_g^2 T^2 \alpha_\lambda}{2\pi}\right)^2 M\left[\ln\left(1+\frac{\gamma^2\Theta_d^2}{1+\gamma^2/\gamma_*^2}\right) - \frac{\gamma^2\Theta_d^2}{1+\gamma^2\Theta_d^2+\gamma^2/\gamma_*^2}\right]. \tag{22}$$

Formulas (22) and (17), where the front half factor may be presented as

$$\frac{e^2|\chi_g|\alpha_\lambda}{8\sin^2(\varphi/2)}\tanh(t_\lambda) = \frac{e^2}{4\pi}\frac{\omega_g^2 T^2\alpha_\lambda}{2\pi}\tanh\left(\frac{\omega_g^2 T^2\alpha_\lambda}{2\pi}M\right), \tag{23}$$

allow us to choose the best suitable conditions for maximizing source emission.

Since $N_\lambda^{DTR} \sim \gamma^4/\gamma_*^4 \ll 1$ if $\gamma < \gamma_*$ in accordance with Eq. (17) and general properties of transition radiation, formula (22) describes correctly the total emission yield from electron beam with energies $m\gamma < m\gamma_*$. DTR's emission angular density contribution may dominate for higher electron energies $m\gamma \gg m\gamma_*$. Indeed, the DTR's angular density is more than PXR's by a factor $\gamma^2/\gamma_*^2 \gg 1$ as may be seen from expressions (17) and (22). Note that the strong difference between the DTR and PXR angular distributions causes a weak interference between these emission mechanisms as our analysis implies.

From Eqs. (22) and (23) DTR and PXR yields are proportional to the number of periods in a multilayer M, if $M < M_{opt} = 2\pi/\omega_g^2 T^2$ [the coefficient $(\omega_g^2 T^2\alpha_\lambda/2\pi)^2$ in Eq. (22) describes the coherent photon reflection by target's electrons, placed at one period of the structure]. For this case N_λ^{PXR} and N_λ^{DTR} are approximately the same for a large angular-size collimator $\Theta_d > \gamma_*^{-1} \gg \gamma^{-1}$. However, in the range $M > M_{opt}$ DTR yield is saturated [Eq. (23)] and PXR can become more efficient for x-ray production.

To estimate the influence of photoabsorption on these processes let us now consider the general solution (12) for semi-infinite target. Our analysis shows that DTR spectral-angular distribution from an absorbing semi-infinite multilayer is described by expression (15), where the quantity

$$R_\lambda^{DTR} = \frac{1}{|\tau_\lambda - i\beta_\lambda + \sqrt{\tau_\lambda - 1 - 2i\beta_\lambda(\tau_\lambda - \sigma_\lambda)}|^2}, \tag{24a}$$

$$\beta_\lambda = \frac{\chi_0''}{|\chi_g|\alpha_\lambda}, \quad \sigma_\lambda = \frac{\sin\left(\pi\frac{a}{T}\right)}{\pi}\frac{\chi_a''-\chi_b''}{\chi_0''}\alpha_\lambda \tag{24b}$$

must be inserted as the reflection coefficient. The reflection coefficients R_λ^{DTR} from Eqs. (24) and (15) for $t_\lambda > 1$ are close to each other, because the coefficient β_λ is usually much smaller than unity (β_λ is the ratio of the extinction length to the absorption one).

Similarly, it is easy to show that the absorption does not change the main PXR properties. The equation, analogous to Eq. (20), has the form

$$\frac{dN_\lambda^{PXR}}{d^2\Theta}=\frac{e^2}{\pi^2}\left(\frac{\omega_g^2 T^2\alpha_\lambda}{2\pi}\right)^2 M_{eff}\left\langle\frac{\Omega_\lambda^2}{(\gamma^{-2}+\gamma_*^{-2}+\Omega^2)^2-2\sigma_\lambda(\gamma^{-2}+\gamma_*^{-2}+\Omega^2)|\chi_g|\alpha_\lambda+|\chi_g|^2\alpha_\lambda^2}\right.$$
$$\left.\times\left(1-\frac{|\chi_g|^2\alpha_\lambda^2}{(\gamma^{-2}+\gamma_*^{-2}+\Omega^2)^2}\right)^2\right\rangle, \tag{25}$$

where M_{eff} is the effective number of multilayer periods making contribution to PXR yield formation,

$$M_{eff}=\frac{\sin^2\left(\frac{\varphi}{2}\right)}{\pi\chi_0''}=\frac{\sin\left(\frac{\varphi}{2}\right)}{\omega_B\chi_0''T}\equiv\frac{L_{ab}\sin\left(\frac{\varphi}{2}\right)}{T}. \tag{26}$$

Thus, the advantage of multilayers as DTR and PXR radiators, following from Eqs. (18) and (21), is preserved for an absorbing target as well.

We performed multilayer experiments using 500-MeV electron beam and a commercially available x-ray multilayer mirror manufactured by OSMIC Inc. [33]. The mirror consisted of 300 pairs of W and B_4C layers with spacing $T=12.36\times10^{-8}$ cm and supported by 100-μm Si substrate. The x rays were emitted at the angle $\varphi=3.8°$ with respect to the electron-beam direction (see Fig. 1). The thicknesses of the layers a and b were the same. X rays generated in the mirror or in its Si substrate were detected by a CdTe semiconductor detector, placed at the distance of 443 cm from the radiator. The detector's aperture was 4 mm^2. Since the angular size of the detector $\Theta_d\approx5\times10^{-4}$ was less than the characteristic emission angle for relativistic electrons $\gamma^{-1}=10^{-3}$, we were able to measure the spectral-angular distribution of emitted photons [33].

Since the measurement of the current of the storage ring's electron beam was not available to us to measure, the x-ray intensity was measured only in arbitrary units and the intensity enhancement in multilayer structure in comparison to crystal could not be demonstrated. On the other hand, since the angular distributions or orientational dependencies of PXR and DTR are very different for the conditions of the experiment, we can determine the main emission mechanism. The ratio γ^2/γ_*^2 determining the difference between PXR and DTR angular distributions is $\approx10\gg1$ for a 500-MeV electron beam.

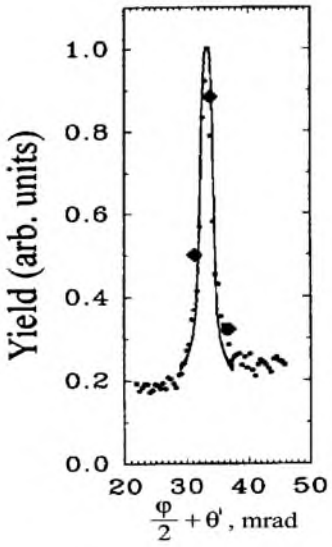

FIG. 2. The comparison of the calculated and measured [33] orientational dependence of the collimated x-ray yield.

The measured orientational dependence of the x rays is presented in Fig. 2. To estimate relative contributions of DTR and PXR to the observed yield we compare the magnitudes of the DTR and PXR angular distributions for the experimental parameters $\sqrt{\langle\omega_p^2\rangle}\approx50$ eV, $\omega_B\approx15$ keV, $\chi_0''(\omega_B)\approx0.9\times10^{-4}$, $M=300$, $\gamma_*=300$. We obtain the following estimations: $(dN_\lambda^{PXR}/d^2\Theta)_{max}\approx6\times10^{-3}$ (photon/e sr) and $(dN_\lambda^{DTR}/d^2\Theta)_{max}\approx0.8$ (photon/e sr). Thus DTR dominates in the measured emission yield.

The theoretical orientational dependence is also presented in Fig. 2 (solid line). It was calculated without a PXR contribution and bremsstrahlung background. The PXR orientational dependence is much wider than that of DTR and cannot explain the experimental data. The calculated curve and experimental data are normalized at one point. As seen in the figure, the calculated curve agrees with data. The comparison of calculated DTR spectra is also in agreement with the measured. Thus, the theory developed in this work is in good agreement with the experimental results [33].

IV. CONCLUSIONS

Our analysis has shown that PXR and DTR are the main emission mechanisms for relativistic electrons passing through a multilayer mirror. The relative contribution of these two mechanisms to total yield depends on the electron's energy. If it is smaller than the critical energy $m\gamma_*=m\omega_B/\sqrt{\langle\omega_p^2\rangle}$, then PXR dominates. The PXR efficiency of a multilayer source can exceed that of a crystal for these lower electron energies. This occurs because a larger number of multilayer's electrons make a coherent contribution to the formation of x rays. The number of emitted x-ray photons is about 10^{-4}–10^{-3} per electron. Crystals are limited to 10^{-6}–10^{-5}.

If the energy of the emitting electron exceeds the critical energy, then the PXR and DTR contributions depend on the target thickness L and the x-ray detector angular size Θ_d. The total emission yield may be determined by PXR contribution if $\Theta_d>\gamma_*^{-1}$ and the radiator is thick enough. On the other hand, DTR dominates if $\Theta_d\leqslant\gamma^{-1}$. Our theory has

been compared with our experimental results and we have shown that the observed x-ray yield is explained by DTR. The efficiency of DTR source was approximately the same as that of PXR radiator: 10^{-4} photons per electron.

The brightness and efficiency of the source can be improved further by using a cyclical accelerator wherein the electron beam is passed through a multilayer many times. In this scheme, a thin multilayer with the period number $M \approx M_{opt}$ would be installed inside the vacuum chamber of a cyclical accelerator such as a betatron [35]. Multipassing of the electron beam through thin crystals has been experimentally demonstrated using a storage ring [36].

Our theoretical and experimental results demonstrate the possibility of making an x-ray source intense enough for medical and other applications [37,38]. The analysis presented in this work allows one to calculate most of the needed characteristics of such a source.

ACKNOWLEDGMENTS

This work was supported by the United States National Institutes for Health under Small Business Innovation Research (SBIR) program (Grant No. 2-R33CA086545-02) and the United States National Science Foundation under the SBIR program (Grant No. DMI-0214819) and by the Russian Foundation of Basic Research (Grant Nos. 02-02-16941 and 03-02-16587).

[1] V.L. Ginzburg and I.M. Frank, J. Phys. (Moscow) **9**, 3533 (1945).
[2] G. M Garibian, Zh. Eksp. Teor. Fiz. **33**, 1403 (1958) [Sov. Phys. JETP **6**, 1079 (1958)].
[3] M.L. Ter-Mikaelian, *High Energy Electromagnetic Processes in Condensed Media* (Wiley, New York, 1972).
[4] A.I. Alikhanian, F.R. Arutyunian, K.A. Ispirian, and M.L. Ter–Mikaelian, Zh. Eksp. Teor. Fiz. **41**, 2002 (1961) [Sov. Phys. JETP **14**, 1421 (1962)].
[5] M.L. Cherry, G. Hartman, D. Muller, and T.A. Prince, Phys. Rev. D **10**, 3594 (1974).
[6] M.A. Piestrup, D.G. Boyers, C.I. Pincus, J.L. Harris, H.S. Caplan, R.M. Silzer, and D.M. Skopik, Appl. Phys. Lett. **59**, 189 (1991).
[7] M.A. Piestrup, D.G. Boyers, C.I. Pincus, J.L. Harris, X.K. Maruyama, J.C. Berystrom, H.S. Caplan, R.M. Silzer, and D.M. Skopik, Phys. Rev. A **43**, 3653 (1991).
[8] Y.B. Fainberg and N.A. Khizhniak, Zh. Eksp. Teor. Fiz. **32**, 883 (1957) [Sov. Phys. JETP **5**, 720 (1957)].
[9] M.L. Cherry, D. Muller, and T.A. Prince, Nucl. Instrum. Methods **115**, 141 (1974).
[10] M.J. Moran, B.A. Dahling, P.J. Ebert, M.A. Piestrup, B.L. Berman, and J.O. Kephart, Phys. Rev. Lett. **57**, 1223 (1986).
[11] M.A. Piestrup, D.G. Boyers, C.I. Pincus, Qiang Li, G.D. Hallewell, M.J. Moran, X.K. Maruyama, D.D. Snyder, R.M. Silzer, D.M. Skopik, and G.B. Rothbart, Phys. Rev. A **45**, 1183 (1992).
[12] N. Zhevago, in *Proceedings of the Second Symposium on Transition Radiation of High Energy Particles* (Yerevan Physics Institute, Yerevan, Armenia, 1983), p. 200.
[13] C.T. Law and A.E. Kaplan, Opt. Lett. **12**, 900 (1987).
[14] B. Pardo and J.-M. Andre, Phys. Rev. A **40**, 1918 (1989).
[15] M.S. Dubovikov, Phys. Rev. A **50**, 2068 (1994).
[16] J.-M. Andre, B. Pardo, and C. Bonnelle, Phys. Rev. E **60**, 968 (1999).
[17] B. Lastdrager, A. Tip, and J. Verhoevan, Phys. Rev. E **61**, 5767 (2000).
[18] B. Pardo and J.-M. Andre, Phys. Rev. E **65**, 036501 (2002).
[19] N.K. Zhevago and V.I. Glebov, Phys. Lett. A **309**, 311 (2003).
[20] V.G. Baryshevsky and I.D. Feranchuk, Zh. Eksp. Teor. Fiz. **61**, 944 (1971) [Sov. Phys. JETP **34**, 502 (1972)].
[21] G.M. Garibian and Yang Shi, Zh. Eksp. Teor. Fiz. **61**, 930 (1971) [Sov. Phys. JETP **34**, 495 (1972)].
[22] V.G. Baryshevsky and I.D. Feranchuk, J. Phys. (Paris) **44**, 913 (1983).
[23] A. Caticha, Phys. Rev. A **40**, 4322 (1989).
[24] Yu.N. Adishchev, S.A. Vorob'ev, B.N. Kalinin, S. Pak, and A.P. Potylitsin, Zh. Eksp. Teor. Fiz. **90**, 829 (1986) [Sov. Phys. JETP **63**, 484 (1986)].
[25] A.V. Shchagin, V.I. Pristupa, and N.A. Khithnyak, Phys. Lett. A **148**, 485 (1990).
[26] K.-H. Brenzinger, C. Herberg, B. Limburg, H. Backe, S. Dambach, H. Euteneuer, F. Hagenbuck, H. Hartmann, W. Schope, and Th. Walcher, Z. Phys. A **358**, 107 (1997).
[27] Y.N. Adischev *et al.*, Nucl. Instrum. Methods Phys. Res. B **201**, 114 (2003).
[28] Z.G. Pinsker, *Dynamic Scattering of X-rays in Crystals* (Springer, Berlin, 1981).
[29] I.D. Feranchuk and A.V. Ivashin, J. Phys. (Paris) **46**, 1981 (1985).
[30] A. Caticha, Phys. Rev. B **45**, 9541 (1992).
[31] X. Artru and P. Rullhusen, Nucl. Instrum. Methods Phys. Res. B **145**, 1 (1998).
[32] N. Nasonov, in *Electron-Photon Interaction in Dense Media*, edited by H. Wiedermann (Kluwer Academic, Dordrecht, 2002), p. 49.
[33] V.V. Kaplin, S.R. Uglov, V.N. Zabaev, M.A. Piestrup, C.K. Gary, and N.N. Nasonov, Appl. Phys. Lett. **76**, 3647 (2000).
[34] A.M. Afanasyev and M.A. Aginian, Zh. Eksp. Teor. Fiz. **74**, 570 (1978) [Sov. Phys. JETP **47**, 300 (1978).
[35] M.Yu. Andreyashkin, V.V. Kaplin, M.A. Piestrup, S.R. Uglov, and V.N. Zabaev, Appl. Phys. Lett. **72**, 1385 (1998).
[36] V.V. Kaplin, S.R. Uglov, O.F. Bulaev, V.J. Goncharov, M.A. Piestrup, and C.K. Gary, Nucl. Instrum. Methods Phys. Res. B **173**, 3 (2001).
[37] M.A. Piestrup, Xizeng Wu, V.V. Kaplin, S.R. Uglov, J.T. Cremer, D.W. Rule, and R.B. Frioito, Rev. Sci. Instrum. **72**, 2159 (2001).
[38] C.K. Gary, M.A. Piestrup, D.G. Boyers, C.I. Pincus, R.H. Pantell, and G.B. Rothbart, Med. Phys. **204**, 1527 (1993).